

Controls on Upper Ocean Enzymatic Nitrate–Nitrite Isotopic Exchange in and beyond Southern Ocean

Yangjun Chen, Min Chen,* and Minfang Zheng



Cite This: *Environ. Sci. Technol.* 2025, 59, 6074–6084



Read Online

ACCESS |



Metrics & More



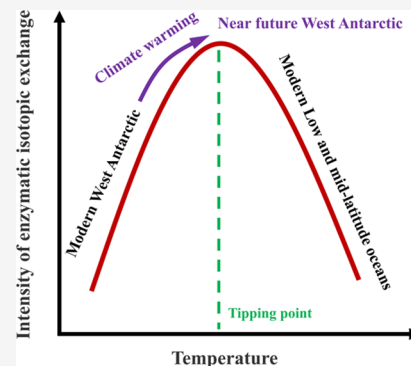
Article Recommendations



Supporting Information

ABSTRACT: Increasing studies have recognized that the enzymatic nitrate–nitrite isotopic exchange reaction may be a potential breakthrough to update our understanding of the nitrogen cycle. However, fundamental aspects of this reaction remain poorly understood, limiting our comprehensive understanding of the nitrogen cycle. In this study, we present the first coupled measurements of nitrate and nitrite dual isotopes at natural abundance across the Antarctic summer to uncover the environmental factors influencing enzymatic isotopic exchange. East Antarctic surface waters exhibit the most anomalous nitrate and nitrite isotope signatures and a more pronounced equilibrium isotope effect compared to West Antarctica. This feature may be attributed to the regulation of enzymatic isotopic exchange reaction by temperature, and we infer that there might be a tipping point in the expression of its intensity. Given the warming of Antarctic waters due to global climate change, particularly in West Antarctic, we hypothesize that such reaction could have an amplified impact on nitrogen isotope dynamics. Further analyses incorporating data from beyond the Southern Ocean also suggest that functional differences in the nitrite oxidoreductase enzyme itself are a critical contributing factor. Overall, our study provides new insights into the mechanisms underlying the enzymatic isotopic exchange reaction, with broad implications for models of the modern upper ocean nitrogen cycle and paleoceanographic reconstructions of ancient nitrogen cycle dynamics.

KEYWORDS: isotopic exchange, antarctica water, nitrite isotopes, temperature dependence, isotopic dynamics, equilibrium isotope effect



1. INTRODUCTION

Nitrogen (N) is a key biogenic element for the growth of all living organisms on Earth. Its cycling, primarily driven by diverse microbial communities, is closely linked to the cycling of other elements such as carbon and phosphorus,¹ playing a significant role in global climate change and the functioning of Earth's ecosystems. To capture the key transformation processes and their interactions within the N cycle network, various approaches have been developed, with stable N and oxygen (O) isotopes being widely and successfully employed.^{2–9} Nitrate (NO_3^-) and nitrite (NO_2^-) are two key forms in the N cycle, and many studies have employed their N and O isotope ratios as tracers to provide invaluable insights into element cycling in ancient, modern, and future Earth's ecosystems, particularly in marine systems.^{2–9} To fully exploit such recorded information, both the typical N transformation processes and their N and O isotopic fractionations must be clarified.

The enzymatic NO_3^- – NO_2^- isotopic exchange reaction (the exchange of N and O atoms between NO_3^- and NO_2^-), a recently recognized and misunderstood process beyond the canonical N cycle processes (e.g., N assimilation, N_2 fixation, nitrification, denitrification, etc.), has profound implications for advancing our understanding of the N cycle.^{2,10–12} This reaction operates at the enzyme level and is believed to be

catalyzed by nitrite oxidoreductase (NXR), a key enzyme of NO_2^- -oxidizing bacteria (NOB).^{2,10–15} The enzymatic isotopic exchange reaction between NO_3^- and NO_2^- occurs due to the reversible expression of NXR, which facilitates the bidirectional microbial oxidation of NO_2^- and reduction of NO_3^- .^{13–15} Although this reaction involves biogeochemical interconversions between NO_3^- and NO_2^- , it appears to differ from canonical N conversion processes in that it does not significantly alter the substrate concentrations (NO_3^- and NO_2^-). Instead, it seems to primarily affect the isotopic distribution between NO_3^- and NO_2^- .^{2,10} Therefore, the enzymatic NO_3^- – NO_2^- isotopic exchange operates more like a microbially mediated “physical” exchange, directly and uniquely impacting the isotopic systematics of N and O.^{2,3,10–12}

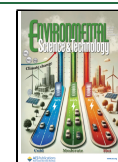
Current single-isotope measurements of oceanic NO_3^- or NO_2^- show specific patterns that differ from those predicted by the canonical N cycle.^{2,3,10,11} The enzymatic NO_3^- – NO_2^-

Received: June 2, 2024

Revised: March 1, 2025

Accepted: March 5, 2025

Published: March 17, 2025



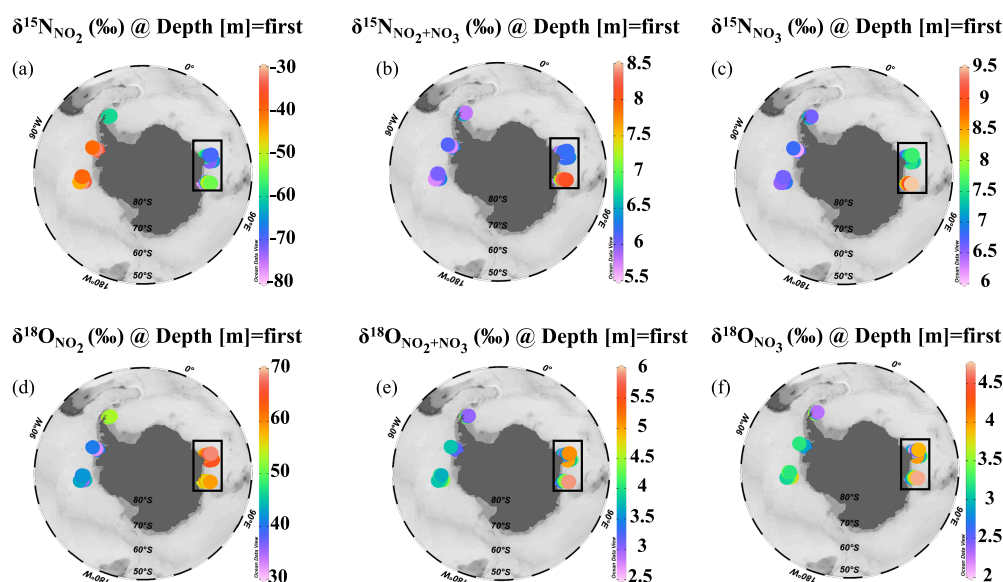


Figure 1. Distribution of dual isotopes of NO_3^- , $\text{NO}_3^- + \text{NO}_2^-$, and NO_2^- in the surface waters of East and West Antarctica. The black boxes indicate sites with the most anomalous isotopic signatures.

isotopic exchange causes distinct changes in the N [$\delta^{15}\text{N} = (^{15}\text{N}/^{14}\text{N}_{\text{Sample}} / ^{15}\text{N}/^{14}\text{N}_{\text{Air}} - 1) \times 1000\text{‰}$] and O [$\delta^{18}\text{O} = (^{18}\text{O}/^{16}\text{O}_{\text{Sample}} / ^{18}\text{O}/^{16}\text{O}_{\text{VSMOW}} - 1) \times 1000\text{‰}$] isotopic compositions of NO_2^- and NO_3^- ,^{2,10,11} especially for NO_2^- , where $\delta^{15}\text{N}_{\text{NO}_2}$ is dramatically reduced and $\delta^{18}\text{O}_{\text{NO}_2}$ is significantly increased.^{2,3} The current understanding of the inverse variations of $\delta^{15}\text{N}_{\text{NO}_2}$ and $\delta^{18}\text{O}_{\text{NO}_2}$ is still limited.^{2,3} Some insights may be derived from the bidirectional reactions involved in the enzymatic $\text{NO}_3^- - \text{NO}_2^-$ isotopic exchange. Generally, microbes preferentially utilize lighter isotopes (e.g., ^{14}N and ^{16}O) over heavier isotopes (e.g., ^{15}N and ^{18}O), resulting in products that are enriched in ^{14}N and ^{16}O relative to the reactants.⁵ For example, during NO_3^- reduction, a normal kinetic isotope effect results in NO_2^- being enriched in ^{14}N and ^{16}O relative to NO_3^- .^{16,17} It is important to note that during the reduction of NO_3^- to NO_2^- , O atoms are partitioned between NO_2^- and NO_3^- . At this branching point, a branching O isotope effect occurs, with ^{18}O preferentially binding to the resulting NO_2^- .¹⁸ Conversely, an inverse kinetic isotope effect in the NO_2^- oxidation results in the residual NO_2^- (reactant) being enriched in ^{14}N and ^{16}O relative to the produced NO_3^- .^{13,18} Accordingly, with the enzymatic isotopic exchange reaction, $\delta^{15}\text{N}_{\text{NO}_2}$ is expected to continuously decrease as NO_2^- becomes enriched in ^{14}N .² For $\delta^{18}\text{O}_{\text{NO}_2}$, the branching O isotope effect in NO_3^- reduction (20–30‰)¹⁹ is greater than the inverse O isotope effect in NO_2^- oxidation (−8‰ to −1‰),¹⁸ leading to a net increase in $\delta^{18}\text{O}_{\text{NO}_2}$.² It is crucial to note that NO_2^- also undergoes O isotope exchange with H_2O . This exchange process alters the $\delta^{18}\text{O}$ of NO_2^- and is influenced by abiotic factors such as pH and temperature.^{4,18} Given the unique alterations in the isotopic compositions of NO_3^- and NO_2^- induced by the enzymatic $\text{NO}_3^- - \text{NO}_2^-$ isotopic exchange,^{2,3,10–12} this reaction may interfere with estimates of N isotope effects in NO_3^- assimilation, affecting reconstructed paleo-variations in upper ocean nutrients and atmospheric carbon dioxide during glacial/interglacial periods.¹¹ Additionally, it may impact biogeochemical models of N turnover and the estimation of global ocean N budget.^{2,3,10–12} The unexplained NO_2^- oxidation in oxygen-deficient zones (ODZs)^{20–26} may also

be attributable to this reaction.¹² Consequently, this reaction challenges the canonical N cycle. However, two crucial questions remain unresolved: whether this reaction occurs in the world's oceans and what environmental factors regulate the N and O isotopic exchange systematics.^{2,3,10–12} The influence of the enzymatic $\text{NO}_3^- - \text{NO}_2^-$ isotopic exchange reaction remains underexplored, limiting its integration into the global N cycle and constraining our understanding of N cycle dynamics in a changing world.

Increasing evidence indicates that enzymatic $\text{NO}_3^- - \text{NO}_2^-$ isotopic exchange occurs in the Southern Ocean mixed layer,^{2,3,10,11} making it an ideal natural laboratory. The mechanisms driving this reaction in the Southern Ocean may offer further insights into the N cycle in low- and mid-latitude oceans. Dual isotopes of NO_2^- are more capable of capturing the signal of enzymatic $\text{NO}_3^- - \text{NO}_2^-$ isotopic exchange but are rarely reported in the Southern Ocean.^{2,3} Here, we present the first large-scale coupled measurements of natural abundances of NO_3^- and NO_2^- dual isotopes across different regions of the Southern Ocean (Figures 1 and S1), aiming to reveal the spatial patterns of enzymatic $\text{NO}_3^- - \text{NO}_2^-$ isotopic exchange and to explore the environmental factors driving its variability. Additionally, we assess whether this reaction is globally widespread by combining NO_2^- isotope data from the surface or mixed layers of the world's oceans.

2. METHODS

2.1. Sampling. Samples were collected from November 2020 to April 2021 onboard the R/V *Xuelong* and R/V *Xuelong* 2 in the East (Weddell Sea, Cosmonaut Sea, and Prydz Bay) and West (Amundsen Sea) Antarctic waters (Figures 1 and S1). A total of 25 sites across 7 transects were sampled. Both NO_3^- and NO_2^- isotope samples were collected from depths of 0–200 m using a Seabird SBE 911 conductivity–temperature–depth (CTD) rosette sampler. NO_3^- isotope samples were collected in 125 mL high-density polyethylene bottles (Nalgene) and acidified with sulfamic acid (1 mL of 2.5 mM sulfamic acid in 25% hydrochloric acid) to remove any measurable NO_2^- and preserve the samples.^{27,28} NO_2^- isotope samples were collected in 250 mL high-density polyethylene

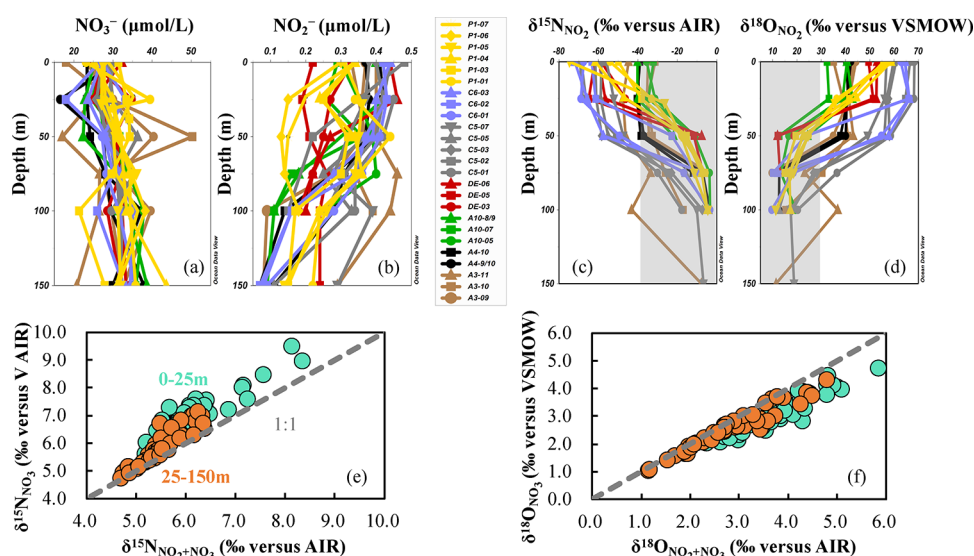


Figure 2. Depth profiles of NO_2^- , NO_3^- , and $\text{NO}_3^- + \text{NO}_2^-$ concentrations, along with their dual isotopes. (a and b) Profiles of NO_2^- and NO_3^- in East (represented by red, gray, blue, and yellow lines) and West Antarctic waters (shown in brown, green, and black lines). (c and d) Profiles of dual isotopes in NO_2^- (concentrations above $0.25 \mu\text{M}$) in East (red, gray, blue, and yellow lines) and West Antarctic waters (brown, green, and black lines). The gray shading represents the range of $\delta^{15}\text{N}_{\text{NO}_2}$ and $\delta^{18}\text{O}_{\text{NO}_2}$ variations attributable to the canonical N cycle (refer to Supporting Information Text S1 for details). (e and f) The relationship between the N and O isotopic compositions of NO_3^- and $\text{NO}_3^- + \text{NO}_2^-$ at various depths. Green represents data from 0 to 25 m, while orange represents data from 25 to 150 m and deeper.

bottles (Nalgene). The pH of these samples was adjusted to 12 by adding 5 to 5.5 mL of 6 M sodium hydroxide to prevent O isotope exchange between NO_2^- and H_2O during storage.^{2,3,8,9,28–30}

2.2. Hydrochemical Analysis. Temperature, salinity, and chlorophyll *a* were directly measured using precalibrated probes equipped on the CTD. Dissolved oxygen (DO) was measured with an SBE oxygen sensor and calibrated against discrete measurements using Winkler titration. Nutrient samples were filtered GF/F filters (47 mm, Whatman) and frozen immediately after collection via CTD. NO_3^- and NO_2^- concentrations were determined using a Four-channel Continuous Flow Technicon Auto-Analyzer III (AA3, Bran-Luebbe, Germany) and a QuAAtro flow analyzer (Seal, Germany) via flow injection technique, employing the Greiss-Ilosvay colorimetric method.³¹ The procedure included reagent preparation (cadmium column, sulfanilamide, and N-(1-naphthyl) ethylenediamine), preparation of primary and secondary standards, and correction for blanks and refractive index. Nutrients were analyzed with a precision of 5% and detection limits of 0.02 and $0.07 \mu\text{mol L}^{-1}$ for NO_3^- and NO_2^- , respectively.³²

2.3. Isotopic Analysis. The $\delta^{15}\text{N}$ and $\delta^{18}\text{O}$ of NO_3^- were determined using the bacterial method.^{33–35} Briefly, samples were first neutralized with sodium hydroxide, then NO_3^- was quantitatively converted into nitrous oxide (N_2O) by cultured denitrifying bacteria lacking N_2O reductase (*Pseudomonas aureofaciens*, ATCC #13985). For NO_2^- isotope analysis, the azide method was employed to reduce NO_2^- to N_2O .³⁶ Due to the detection limit of this method, only samples with NO_2^- concentrations exceeding $0.25 \mu\text{mol/L}$ were used to determine $\delta^{15}\text{N}$ and $\delta^{18}\text{O}$ of NO_2^- .^{2,3,8,9} Given the high pH of the samples, the concentration of acetic acid was increased to 7.84 M to ensure effective NO_2^- reductions.^{2,3,8,9,29} To maximize the yield of N_2O , 10 mL of each sample was transferred to a headspace vial for reactions.^{2,3,8,9} To avoid interference from N_2O potentially present in the sample, all sample solutions

were purged with high-purity helium. The $\delta^{15}\text{N}$ and $\delta^{18}\text{O}$ of $\text{NO}_3^- + \text{NO}_2^-$ were calculated from the measured concentrations and isotopic compositions of NO_3^- and NO_2^- using an isotope mass balance.

The isotopic composition of N_2O was automatically extracted, purified, concentrated and analyzed online using a Thermo Finnigan Gasbench II purge-trap system interfaced with a DELTA^{plus} XP isotope ratio mass spectrometer. The isotopic standards for NO_3^- (USGS-34: $\delta^{15}\text{N} = -1.8\text{‰}$, $\delta^{18}\text{O} = -27.9\text{‰}$; IAEA-N3: $\delta^{15}\text{N} = 4.7\text{‰}$, $\delta^{18}\text{O} = 25.6\text{‰}$ ³⁴ and two in-house reference materials LAB-Mix1: $\delta^{15}\text{N} = 89.3\text{‰}$, $\delta^{18}\text{O} = -1\text{‰}$; LAB-Mix2: $\delta^{15}\text{N} = 14.6\text{‰}$, $\delta^{18}\text{O} = -23.09\text{‰}$) and for NO_2^- (RSIL-N23: $\delta^{15}\text{N} = 3.7\text{‰}$, $\delta^{18}\text{O} = 11.4\text{‰}$; RSIL-N7373: $\delta^{15}\text{N} = -79.6\text{‰}$, $\delta^{18}\text{O} = 4.5\text{‰}$; RSIL-N10219: $\delta^{15}\text{N} = 2.8\text{‰}$, $\delta^{18}\text{O} = 88.5\text{‰}$)¹⁸ were preserved and processed in the same procedure as the samples to calibrate the isotope values. Specifically, the slope of the NO_2^- isotopic standard curves, prepared using the same water,³⁰ ranged from 0.82 ± 0.01 ($\delta^{18}\text{O}_{\text{N}_2\text{O-measured}}$ VS $\delta^{18}\text{O}_{\text{NO}_2\text{-known}}$) to 0.49 ± 0.01 ($\delta^{15}\text{N}_{\text{N}_2\text{O-measured}}$ VS $\delta^{15}\text{N}_{\text{NO}_2\text{-known}}$) for NO_2^- concentrations of $0.5\text{--}1 \mu\text{M}$, and 0.80 ± 0.01 to 0.47 ± 0.01 for $0.25\text{--}0.5 \mu\text{M}$. The reaction solution volume for each sample and standard was kept constant to minimize possible pH dependence in the azide reduction reaction and the effect of solution volume on the purge and trap procedures to recover analyte N_2O .^{30,37} The N content of the standards was matched to the samples to minimize the effect of sample size on $\delta^{15}\text{N}$ and $\delta^{18}\text{O}$ analyses.^{30,37} The mean standard deviations for all replicate measurements of samples and standards in this study were 0.3‰ for $\delta^{15}\text{N}$ and 0.4‰ for $\delta^{18}\text{O}$, respectively.

3. RESULTS

3.1. Nitrite and Nitrate Dual Isotopes. Compared to the upper ocean in mid- and low-latitudes, nutrient concentrations in the upper Southern Ocean are relatively higher (Figures 2a, 2b and S2), likely due to limitations in light³⁸ or iron.³⁹ As a result, simultaneous measurements of N and O isotopes of

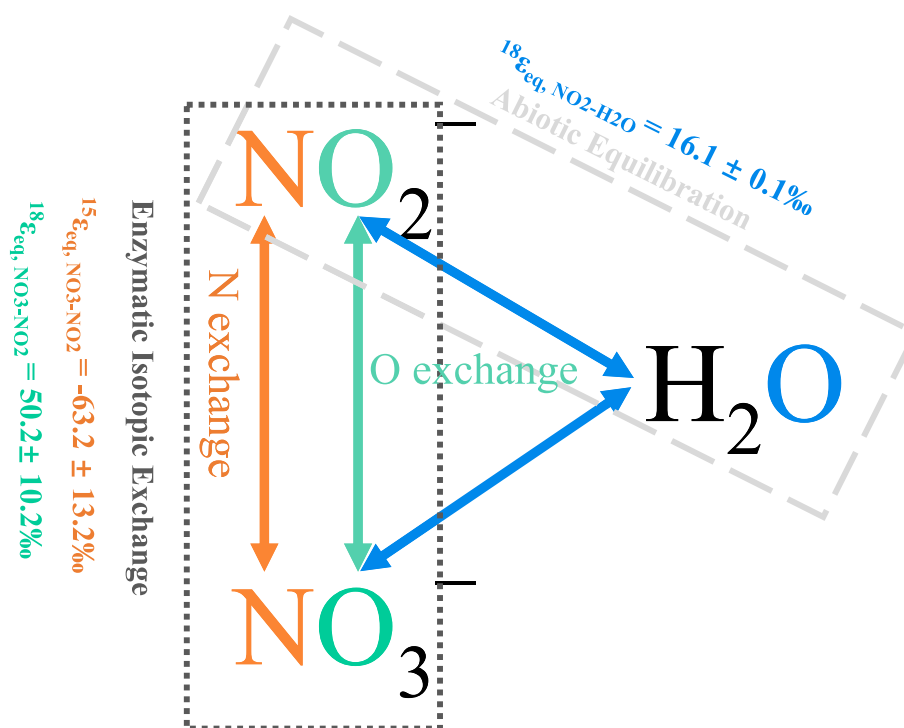


Figure 3. Exchange and fractionation effects of N and O isotopes in enzymatic $\text{NO}_3^- - \text{NO}_2^-$ isotopic exchange. The light gray box illustrates the O isotope exchange between NO_2^- and ambient H_2O molecules (abiotic equilibration), occurring concurrently with the enzymatic $\text{NO}_3^- - \text{NO}_2^-$ isotopic exchange reaction (dark gray).

NO_2^- and NO_3^- are feasible in this region. Our results show that surface NO_2^- in different sectors of the Southern Ocean exhibits extremely low $\delta^{15}\text{N}_{\text{NO}_2}$ and anomalously high $\delta^{18}\text{O}_{\text{NO}_2}$ (Figures 1a, 1d, 2c, and 2d). The average values of $\delta^{15}\text{N}_{\text{NO}_2}$ in the surface waters of the Amundsen Sea, Weddell Sea, Cosmonaut Sea and Prydz Bay are $-37.2 \pm 4.5\text{‰}$, $-60 \pm 1.7\text{‰}$, $-64.6 \pm 5.7\text{‰}$, and $-65.7 \pm 12.1\text{‰}$ respectively, and the average values of $\delta^{18}\text{O}_{\text{NO}_2}$ are $39.8 \pm 4.1\text{‰}$, $52.4 \pm 2.7\text{‰}$, $63.0 \pm 3.8\text{‰}$, and $56.2 \pm 2.6\text{‰}$, respectively. These values are significantly anomalous compared to the $\delta^{15}\text{N}_{\text{NO}_2}$ (-38‰ to 0‰) and $\delta^{18}\text{O}_{\text{NO}_2}$ (3.3‰ to 23.9‰) reported in the majority of the upper ocean.^{2,4,8,9,22,40–48} Furthermore, we also estimate the theoretical extremes of $\delta^{15}\text{N}_{\text{NO}_2}$ (-39.8‰) and $\delta^{18}\text{O}_{\text{NO}_2}$ (29.2‰) in the upper ocean based on the canonical N cycle framework and associated isotope effects (The gray shading in Figure 2c, 2d, see support information for details). However, these theoretical extremes fail to explain the observed NO_2^- isotopic anomalies (The gray shading in Figure 2c, 2d). Clearly, our results are consistent with the previously reported $\delta^{15}\text{N}_{\text{NO}_2}$ (as low as -90‰) and $\delta^{18}\text{O}_{\text{NO}_2}$ (as high as 63.3‰) in the Southern Ocean,^{3,11} where such anomalies have been attributed to enzymatic $\text{NO}_3^- - \text{NO}_2^-$ isotopic exchange reaction.^{2,3,10,11} In fact, this reaction provides the most plausible explanation, as it can impart extremely low $\delta^{15}\text{N}$ and anomalously high $\delta^{18}\text{O}$ to NO_2^- ,^{2,3,10,11} which is fully consistent with the signals we observed.

Interestingly, these anomalous isotopic signals in NO_2^- show spatial variations in East (Weddell Sea, Cosmonaut Sea, and Prydz Bay) and West Antarctica (Amundsen Sea), with larger anomalies in the former (Figure 1a, 1d). Similarly, the $\delta^{15}\text{N}$ and $\delta^{18}\text{O}$ of NO_3^- and $\text{NO}_3^- + \text{NO}_2^-$ are significantly different in the surface waters of West and East Antarctica (Figure 1). In East Antarctic surface waters, the $\delta^{15}\text{N}$ of NO_3^- is higher than that of $\text{NO}_3^- + \text{NO}_2^-$, and the difference in $\delta^{18}\text{O}$

between the two is most significant, which is consistent with the large anomalies of $\delta^{15}\text{N}$ and $\delta^{18}\text{O}$ in NO_2^- observed in East Antarctica (Figure 1).

With increasing depth, the $\delta^{15}\text{N}_{\text{NO}_2}$ value gradually increased to $-3.4 \pm 0.5\text{‰}$, while the $\delta^{18}\text{O}_{\text{NO}_2}$ decreased to $9.6 \pm 0.6\text{‰}$ (Figure 2c, 2d). These values are distinctly different from those at the surface and fall within the range indicative of the canonical N cycle,^{2,10} suggesting that surface anomalies have not persisted (Figure 2c, 2d). This gradual disappearance of NO_2^- isotope anomalies with depth is consistent across both East and the West Antarctic waters, with no discernible differences (Figure 2c, 2d). Similarly, the $\delta^{15}\text{N}$ and $\delta^{18}\text{O}$ differences between NO_3^- and $\text{NO}_3^- + \text{NO}_2^-$ also decrease with depth (Figure 2e, 2f), consistent with the disappearance of NO_2^- isotopic anomalies at greater depths (Figure 2c, 2d). The isotope profile observed implies a transition from a state of strong enzymatic $\text{NO}_3^- - \text{NO}_2^-$ isotopic exchange at the surface to one dominated by canonical N cycle processes.

3.2. Isotope Systematics. To understand the N and O isotope systematics in the enzymatic $\text{NO}_3^- - \text{NO}_2^-$ isotopic exchange, we estimate the equilibrium N and O isotope effects ($^{15}\epsilon_{\text{eq}, \text{NO}_2-\text{NO}_3} = [({}^{15}\text{N}/{}^{14}\text{N})_{\text{NO}_2}/({}^{15}\text{N}/{}^{14}\text{N})_{\text{NO}_3} - 1] \times 1000\text{‰}$) and $^{18}\epsilon_{\text{eq}, \text{NO}_2-\text{NO}_3} = [({}^{18}\text{O}/{}^{16}\text{O})_{\text{NO}_2}/({}^{18}\text{O}/{}^{16}\text{O})_{\text{NO}_3} - 1] \times 1000\text{‰}$) based on a reported approach that assumes isotopic exchange between surface NO_3^- and NO_2^- is in equilibrium.² The estimated $^{15}\epsilon_{\text{eq}, \text{NO}_2-\text{NO}_3}$ and $^{18}\epsilon_{\text{eq}, \text{NO}_2-\text{NO}_3}$ values for the Amundsen Sea, Weddell Sea, Cosmonaut Sea, and Prydz Bay are $-43.8 \pm 4.6\text{‰}$ and $36.6 \pm 3.9\text{‰}$, $-67.0 \pm 1.7\text{‰}$ and $49.5 \pm 2.5\text{‰}$, $-73.2 \pm 5.1\text{‰}$ and $60.8 \pm 2.8\text{‰}$, $-68.8 \pm 10.4\text{‰}$ and $53.8 \pm 1.5\text{‰}$, respectively. The average values of $^{15}\epsilon_{\text{eq}, \text{NO}_2-\text{NO}_3}$ and $^{18}\epsilon_{\text{eq}, \text{NO}_2-\text{NO}_3}$ in Antarctic waters are $-63.2 \pm 13.2\text{‰}$ and $50.2 \pm 10.2\text{‰}$, respectively. The estimation of $^{15}\epsilon_{\text{eq}, \text{NO}_2-\text{NO}_3}$ is very close to the theoretical value derived from the molecular vibration frequencies of ^{15}N -

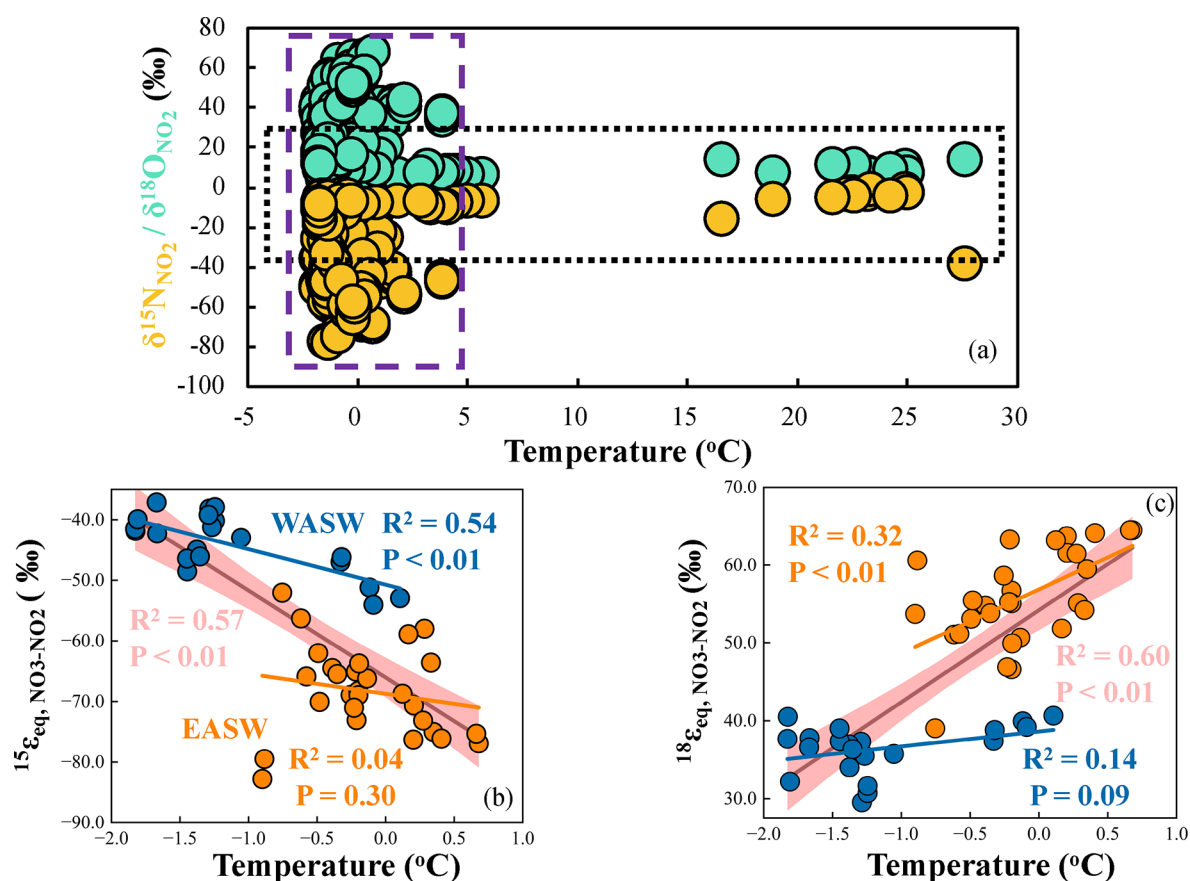


Figure 4. Effect of temperature on N and O isotopic exchange in the NO_3^- - NO_2^- system in Antarctic waters. Panel a illustrated the relationship between $\delta^{15}\text{N}_{\text{NO}_2}$ and $\delta^{18}\text{O}_{\text{NO}_2}$ with temperature in the mixed layer of the global oceans. The purple box indicates the temperature range where NO_2^- isotopes exhibit abnormal behavior (from -1.8 to 3.8 °C). The black box represents the variation range of $\delta^{15}\text{N}_{\text{NO}_2}$ and $\delta^{18}\text{O}_{\text{NO}_2}$ as defined by the canonical nitrogen cycle.^{2,10} Data for Antarctic and Arctic waters are sourced from this study and our previous research,^{2,9} while data for mid- and low-latitude waters are from other reports.^{4,5,17,18,57,59–61} Panel b shows $^{15}\epsilon_{\text{eq}, \text{NO}_2-\text{NO}_3}$ against temperature for East and West Antarctic waters, and panel c shows $^{18}\epsilon_{\text{eq}, \text{NO}_2-\text{NO}_3}$ against temperature for the same regions. WASW and EASW denote East Antarctic and West Antarctic surface waters, respectively.

and ^{14}N -bearing NO_3^- and NO_2^- at 0 °C ($^{15}\epsilon_{\text{eq}, \text{NO}_2-\text{NO}_3} = -63.6 \pm 4.9\text{‰}$),¹⁰ supporting the reliability of our calculations. According to our estimations, the value of the $^{18}\epsilon_{\text{eq}, \text{NO}_2-\text{NO}_3}$ is smaller than the $^{15}\epsilon_{\text{eq}, \text{NO}_2-\text{NO}_3}$, which is attributed to differences in the way N and O isotopes are exchanged (Figure 3). Unlike the isotopic exchange of N, which is limited to NO_3^- and NO_2^- ,^{2,10} the exchange of O atoms also occurs simultaneously with ambient H_2O molecules, incorporating ^{18}O -depleted atoms. This results in the estimated $^{18}\epsilon_{\text{eq}, \text{NO}_2-\text{NO}_3}$ being an “apparent” isotope effect, with its magnitude being less than $^{15}\epsilon_{\text{eq}, \text{NO}_2-\text{NO}_3}$.² Note that the estimated $^{15}\epsilon_{\text{eq}, \text{NO}_2-\text{NO}_3}$ is negative, while the $^{18}\epsilon_{\text{eq}, \text{NO}_2-\text{NO}_3}$ is positive, indicating that the enzymatic NO_3^- - NO_2^- isotopic exchange reaction will modify the $\delta^{15}\text{N}$ and $\delta^{18}\text{O}$ of NO_3^- or NO_2^- in opposite directions (Figure 3).² This behavior is distinctly different from the isotope effects typically observed in canonical N cycle processes, which generally exhibit consistent directional trends.⁴⁹ For example, during the oxidation of NO_2^- , N and O isotope effects lead to a simultaneous reduction in the isotopic values of $\delta^{15}\text{N}_{\text{NO}_2}$ and $\delta^{18}\text{O}_{\text{NO}_2}$.^{13,18} Similarly, during the reduction of NO_3^- , N and O isotope effects result in a simultaneous increase in the isotopic values of residual NO_3^- .^{16,17} This contrast underscores the distinctive nature of enzymatic isotope exchange in altering the isotopic composition of NO_2^- and NO_3^- ,

distinguishing it from other N cycle processes.⁴⁹ For the reverse modification of NO_2^- and NO_3^- dual isotopes, this may relate to the combined effects of N and O isotope effects occurring during two N transformation processes involved in enzymatic isotopic exchange reaction.²

The $^{15}\epsilon_{\text{eq}, \text{NO}_2-\text{NO}_3}$ and $^{18}\epsilon_{\text{eq}, \text{NO}_2-\text{NO}_3}$ in the Weddell Sea, Cosmonaut Sea, and Prydz Bay in East Antarctica are close to each other, but they are larger than the values in the Amundsen Sea in West Antarctica. This spatial heterogeneity indicates differences in the processes controlling the NO_2^- cycle in East and West Antarctic, providing valuable insights into regional variations in isotope dynamics and serving as tracers for unraveling the complex interactions of the N cycle. Considering that the $^{15}\epsilon_{\text{eq}, \text{NO}_2-\text{NO}_3}$ and $^{18}\epsilon_{\text{eq}, \text{NO}_2-\text{NO}_3}$ obtained in this study in the Amundsen Sea are similar to previous findings in the same region,² it indicates a stable expression of enzymatic NO_3^- - NO_2^- isotopic exchange reaction in specific ocean regions.

4. DISCUSSION

4.1. Environmental Controls on Enzymatic NO_3^- - NO_2^- Isotopic Exchange. Our combined measurements of NO_3^- and NO_2^- isotopes reveal the presence of enzymatic isotopic exchange reaction in both East and West Antarctica, albeit with spatial variability. Despite the significance of this

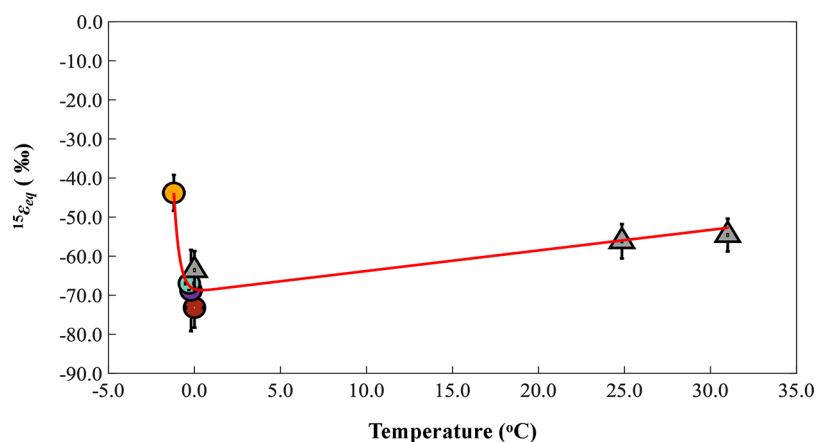


Figure 5. The relationship between $^{15}\epsilon_{eq, NO_2-NO_3}$ and temperature in the enzymatic $NO_3^- - NO_2^-$ isotopic exchange reaction, showing the transition temperature threshold. The circles represent the average $^{15}\epsilon_{eq, NO_2-NO_3}$ values derived from measurements in the Amundsen Sea (yellow), Weddell Sea (light cyan), Cosmonaut Sea (red), and Prydz Bay (purple). The triangles denote the theoretically calculated $^{15}\epsilon_{eq, NO_2-NO_3}$ values based on the molecular vibration frequencies of ^{15}N - and ^{14}N -bearing NO_3^- and NO_2^- at different temperatures.¹⁰ The red curve represents the fitted line, and the black line shows the error bars.

intriguing and complex N cycle process, the environmental regulation of this bidirectional exchange remains unclear.^{2,3,10–12} Some studies suggest that the reversible expression of NXR prefers low pH⁵⁰ and reducing environments,^{13–15} but this is inconsistent with the environmental characteristics of the upper waters in East and West Antarctica. Therefore, understanding which environmental factors regulate the expression of NXR reversibility in East and West Antarctic surface waters is essential.

Previous studies in the Southern Ocean have identified light as a possible environmental factor mediating the enzymatic $NO_3^- - NO_2^-$ isotopic exchange.^{2,10,11} When the mixed layer deepens seasonally, NOB that was originally active in the deeper layers is transported to the mixed layer, where it is inhibited by light, thereby stimulating the NXR-catalyzed $NO_3^- - NO_2^-$ isotopic exchange reaction.¹⁰ A later study suggested that short-term changes in mixed layer depth may be more effective in transporting nitrifiers from deeper layers.¹¹ Additionally, as sea ice melts, nitrifiers that originally lived in the sea ice and adapted to low-light environment are introduced into the ambient water and exposed to stronger light, stimulating the reversible expression of NXR and facilitating enzymatic $NO_3^- - NO_2^-$ isotopic exchange.¹¹ The relationship between NO_2^- isotope anomalies and light also indicated that a high-light environment may be more conducive to this reaction.² If light is indeed the key environmental factor, it would be expected that stronger or weaker expressions of this reaction would be observed in mixed-layer waters throughout the world's oceans, where photoinhibition of nitrifying organisms is present.^{51–54} However, we have not observed the presence of enzymatic $NO_3^- - NO_2^-$ isotopic exchange in surface waters or mixed layers at mid- and low-latitudes (see below), suggesting that light may not be the key environmental regulator of this reaction.

Although our findings suggest a potential link between DO and NO_2^- isotope anomalies, such as more pronounced NO_2^- isotope anomalies at high DO and similar spatial variations in isotopic anomalies and DO (Figures 1, S2 and S3), this contradicts the idea that NXR may favor DO-limited conditions to exhibit its reversibility^{13–15} and thus stimulate an enzymatic isotopic exchange reaction.¹² This implies that

the role of DO in enzymatic isotopic exchange reaction may need to be seriously considered in ODZs.¹² Therefore, the operation of enzymatic isotopic exchange reaction in the upper Southern Ocean must be regulated by other key factors. However, no significant relationships were observed between $^{15}\epsilon_{eq, NO_2-NO_3}$ or $^{18}\epsilon_{eq, NO_2-NO_3}$ and nutrients, salinity and chlorophyll *a* (Figures S2 and S3).

Temperature may be a crucial environmental variable regulating the enzymatic $NO_3^- - NO_2^-$ isotopic exchange. The relationship between dual isotopes in NO_2^- and temperature in various oceanic regions shows that isotopic anomalies only occur in low-temperature environments (−1.8 to 3.8 °C), reflecting the connection between temperature and enzymatic isotopic exchange (Figure 4a). Additionally, the relationship between $^{15}\epsilon_{eq, NO_2-NO_3}$ (or $^{18}\epsilon_{eq, NO_2-NO_3}$) and temperature in different sectors of the Southern Ocean further illustrates that, within the low-temperature range, the enzymatic $NO_3^- - NO_2^-$ isotopic exchange reaction may be enhanced with increasing temperature (Figure 4b, 4c). Further analysis of the theoretically calculated $^{15}\epsilon_{eq, NO_2-NO_3}$ ¹⁰ and the $^{15}\epsilon_{eq, NO_2-NO_3}$ we obtained in the Southern Ocean shows that $^{15}\epsilon_{eq, NO_2-NO_3}$ decreases with increasing temperature under higher temperature scenarios (Figure 5), consistent with the mid- and low-latitude ocean temperature ranges where no isotopic anomalies are observed (Figure 4a). The relationship between $^{15}\epsilon_{eq, NO_2-NO_3}$ and temperature changes at higher and lower temperatures, indicating a tipping point for the enzymatic $NO_3^- - NO_2^-$ isotopic exchange (Figure 5). According to the fitting equation: $^{15}\epsilon_{eq, NO_2-NO_3} = -69.14 \cdot e^{-0.0079t} + 0.6858 \cdot e^{-3.029t}$ (*t*: measured temperature) (Figure 5), we estimate the temperature threshold for this reaction to be approximately 0.44 °C. While this value serves as a useful reference point for understanding this reaction, it should be interpreted with caution due to inherent uncertainties stemming from the limitations of the data set and the assumptions employed in the estimation. Nevertheless, our analysis suggests that the actual threshold likely falls within a similar range, providing meaningful insights into the temperature dependence of the enzymatic isotopic exchange reaction.

Due to the more complex O isotopic systematics compared to N, no $^{18}\epsilon_{eq, NO_2-NO_3}$ values have been reported at different

temperatures, especially at high temperatures. As shown in $^{15}\epsilon_{eq, NO_2-NO_3}$ above, there is a temperature threshold for enzymatic $NO_3^- - NO_2^-$ isotopic exchange. Therefore, it is reasonable to expect that $^{18}\epsilon_{eq, NO_2-NO_3}$ may decrease with increasing temperature in high-temperature environments. This seems plausible. The O isotope exchange between NO_2^- and H_2O is a purely thermodynamic equilibrium process, and its $^{18}\epsilon_{eq, NO_2-H_2O}$ only depends on abiotic factors such as temperature and pH.⁴ Therefore, the trend of $^{18}\epsilon_{eq, NO_2-H_2O}$ is easier to predict than that of $^{18}\epsilon_{eq, NO_2-NO_3}$ in the enzymatic $NO_3^- - NO_2^-$ isotopic exchange reaction. In fact, according to the fitting equation given by Buchwald and Casciotti (2013), $^{18}\epsilon_{eq, NO_2-H_2O}$ will decrease at higher temperatures at fixed pH.⁴ Figure 4a and 4b show that due to the interference of $^{18}\epsilon_{eq, NO_2-H_2O}$, the change of $^{18}\epsilon_{eq, NO_2-NO_3}$ is smaller than that of $^{15}\epsilon_{eq, NO_2-NO_3}$. However, since the temperature rises only in a narrow range (Figure 4c), the decrease in $^{18}\epsilon_{eq, NO_2-H_2O}$ is small and thus has a limited impact on $^{18}\epsilon_{eq, NO_2-NO_3}$. If the temperature rises significantly, the O isotope exchange between NO_2^- and H_2O will become more pronounced,⁴ thereby amplifying its impact on the $\delta^{18}O_{NO_2}$ produced by the enzymatic $NO_3^- - NO_2^-$ isotopic exchange. This may result in a decrease in the $\delta^{18}O_{NO_2}$ since $^{18}\epsilon_{eq, NO_2-NO_3}$ is much larger than $^{18}\epsilon_{eq, NO_2-H_2O}$, and $^{18}\epsilon_{eq, NO_2-H_2O}$ further decreases at higher temperatures.⁴ Consequently, the estimated apparent $^{18}\epsilon_{eq, NO_2-NO_3}$ could be expected to decrease. This aligns with the established relationship between $^{15}\epsilon_{eq, NO_2-NO_3}$ and temperature (Figure 5), providing further validation that the expression of enzymatic $NO_3^- - NO_2^-$ isotopic exchange shifts in response to temperature changes.

To provide a feasible explanation for the observed tipping point in the expression intensity of the enzymatic isotopic exchange reaction, we propose a framework based on the isotopic behavior of sulfur and O in intracellular sulfate.^{12,55} This framework suggests that the reversibility of metabolic pathways regulates the net isotopic fractionation ($^{34}\epsilon_{net}$), which reflects the combined influence of the kinetic isotope effect ($^{34}\epsilon_{kin}$) and the isotopic equilibrium between reactants and products as dictated by thermodynamics ($^{34}\epsilon_{eq}$). The relationship can be described by the following equation:⁵⁵

$$^{34}\epsilon_{net} = (^{34}\epsilon_{eq} - ^{34}\epsilon_{kin}) \times f + ^{34}\epsilon_{kin} \quad (1)$$

where the f represents the ratio of the forward to the reverse reaction in a reversible process. This ratio indicates the degree of reversibility of the reaction, ranging from 0 (indicating an irreversible transformation) to 1 (representing equilibrium between reactants and products, i.e., complete reversibility).⁵⁵ When the net reaction rate of an enzyme-catalyzed reaction is limited (as f approaches 1), the net isotope effect in the enzymatic reaction will approximate the $^{34}\epsilon_{eq}$. Conversely, when the net reaction is unrestricted (as f approaches 0), it tends to reflect the $^{34}\epsilon_{kin}$.⁵⁵ The known reversibility of NXR implies that its reversible activity may generate isotopic dynamics analogous to the sulfur and O isotopic fractionation observed in intracellular sulfate-related processes.^{12,55} Accordingly, the estimated $^{15}\epsilon_{eq, NO_2-NO_3}$ aligns closely with the theoretical $^{15}\epsilon_{eq, NO_2-NO_3}$ at 0 °C (Figure 5), indicating that the enzymatic isotopic exchange reaction is nearly fully reversible (f approaches 1). However, as the temperature decreases further, the estimated $^{15}\epsilon_{eq, NO_2-NO_3}$ begins to deviate (Figure 5). Instead of increasing in magnitude as predicted by theoretical calculations,¹⁰ it starts to decline, resulting in a

tipping point (Figure 5). This characteristic is likely related to changes in the relative expression of intrinsic kinetic isotope effects and the isotopic equilibrium between reactants and products governed by thermodynamics (i.e., deviations of f from 1).⁵⁵ At this stage, the net isotope effect tends toward the kinetic isotope effect. However, since the magnitude of the kinetic isotope effect (for instance, the kinetic N isotope effect during NO_2^- oxidation is -12.8%)^{13,18} is smaller than that of the $^{15}\epsilon_{eq, NO_2-NO_3}$ (-69.2% - -51.4%),¹⁰ the overall magnitude of the net isotope effect is expected to decrease. Therefore, the occurrence of the tipping point is closely associated with changes in f . According to the flux–force relationship, f can be associated with the thermodynamic forces of chemical transformations:⁵⁵

$$f = e^{\Delta G_r/RT} \quad (2)$$

where R represents the gas constant, T denotes the temperature at which the chemical transformation occurs, and ΔG_r indicates the actual free energy change associated with the specific chemical transformation.⁵⁵ It can be observed that the variation of f is related to temperature, suggesting that the occurrence of the tipping point may be temperature-dependent. Furthermore, the isotope effect of enzyme-catalyzed reactions may represent a nonlinear polynomial function of the overall enzymatic reaction rate, with the polynomial coefficients corresponding to the number of steps within the metabolic pathway.⁵⁵ This implies that the complexity of the metabolic process is reflected in the mathematical representation of reaction rates. From a mathematical perspective, enzymatic reactions are inherently temperature-sensitive, with activity typically exhibiting a linear response within specific temperature ranges.^{56–59} However, deviations from linearity occur beyond these ranges due to thermal stress or enzymatic instability, indicating the presence of a critical temperature threshold.^{56–59} This threshold likely represents a tipping point in microbial physiology, characterized by significant changes in metabolic efficiency or enzymatic performance, thereby highlighting the intricate interplay between temperature and microbial activity.^{56–59} These observations suggest that temperature not only modulates enzymatic reaction dynamics but also potentially governs the metabolic adaptability of microbes under varying thermal conditions. Nevertheless, further investigation is required to understand the mechanistic underpinnings of this temperature-dependent behavior, particularly in the context of complex enzyme-catalyzed pathways.

Collectively, the expression of enzymatic $NO_3^- - NO_2^-$ isotopic exchange reaction may be regulated by temperature, with a tipping point in intensity occurring at a specific threshold. Identifying this tipping point holds significant implications for future studies of the N cycle in the Southern Ocean, as it is likely to be reached under ongoing warming.^{60–66} We hypothesize that this reaction may intensify in the near future under scenarios of moderate global warming,⁶⁶ with changes in West Antarctic waters likely to be faster than in East Antarctic waters due to faster warming rates in the former.^{61–65}

4.2. An evaluation of $NO_3^- - NO_2^-$ isotopic exchange in global upper oceans. The question of whether enzymatic $NO_3^- - NO_2^-$ isotopic exchange is ubiquitous in the global upper ocean remains unanswered. Considering that $\delta^{15}N_{NO_2}$ and $\delta^{18}O_{NO_2}$ can better capture the signal of this reaction, we collected and compared isotope data of NO_2^- reported in the

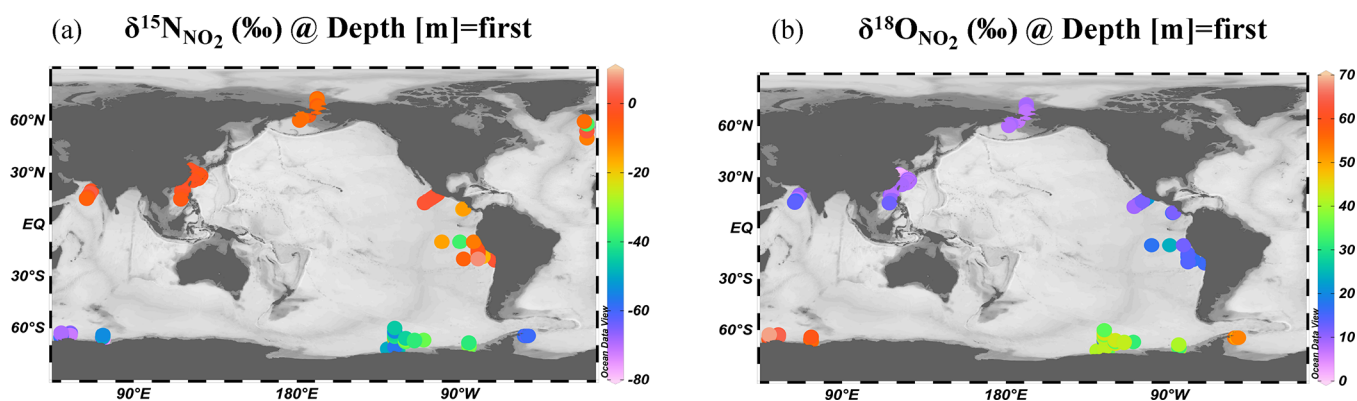


Figure 6. Distribution of $\delta^{15}\text{N}_{\text{NO}_2}$ and $\delta^{18}\text{O}_{\text{NO}_2}$ in the surface/mixed layer of the global ocean. Data for Antarctic and Arctic waters are sourced from this study and our previous work.^{2,9} Data for mid- and low-latitude waters are adapted from various sources, including studies from the East China Sea,⁴¹ South China Sea,⁸ Arabian Sea,^{4,48} subarctic North Atlantic,⁴³ eastern tropical North Pacific,^{21,46} and eastern tropical South Pacific.^{22,29,40,44,45,47} Note that the data from the mixed layer are plotted on the surface for enhanced visualization and comparison.

global ocean to provide an initial evaluation of this issue (Figure 6).^{2,4,8,9,22,40–48} Except for the primary NO_2^- maximum layer, NO_2^- concentrations in other oceanic mixed layers are generally low.^{2,4,8,9,41,42,67,68} Therefore, the NO_2^- isotope data were generally obtained at the primary NO_2^- maximum.^{2,4,8,9,22,40–48} Our data from various regions of the Southern Ocean indicate that $\delta^{15}\text{N}_{\text{NO}_2}$ and $\delta^{18}\text{O}_{\text{NO}_2}$ are still influenced by enzymatic isotope exchange reaction at depths of up to 50 m (Figure 2c and d). This influence may extend to depths of up to 100 m, as suggested by previous studies.^{2,3} This suggests that if similar conditions exist in other ocean regions, the isotopic composition of NO_2^- at depths of 0–100 m should capture the signal of enzymatic isotopic exchange. However, the range of reported values of $\delta^{15}\text{N}_{\text{NO}_2}$ (−38‰ to 0‰) and $\delta^{18}\text{O}_{\text{NO}_2}$ (3.3‰ to 23.9‰) in other oceanic regions can be explained by canonical N cycle processes and their isotope effects.^{2,4,8,9,22,40–48} Thus, we only observe anomalies in $\delta^{15}\text{N}_{\text{NO}_2}$ and $\delta^{18}\text{O}_{\text{NO}_2}$ in the upper waters of the Antarctic, highlighting the uniqueness of the Southern Ocean (Figure 6).

The low-temperature characteristic of the Southern Ocean is significantly distinct from the relatively higher temperatures in mid- and low-latitude oceans (Figure S2). This temperature disparity could account for the weaker or absent enzymatic isotopic exchange in mid- and low-latitude regions, as lower temperatures are likely more conducive to promoting this reaction (Figures 4 and 5). It is important to highlight that, in tropical ODZs, the temperature dependence of the enzymatic isotopic exchange requires careful consideration, as the reversible expression of NXR tends to favor reductive environments.^{13–15} This suggests that oxygen limitation may also play a significant role in the enzymatic isotopic exchange reaction within these ODZs.¹² Therefore, a thorough examination of the mechanisms of this reaction under varying environmental conditions is crucial to further understanding its driving factors.

For the low-temperature Arctic Ocean, the available data do not indicate the occurrence of enzymatic $\text{NO}_3^- - \text{NO}_2^-$ isotopic exchange reaction (Figure 6). Although Arctic waters are cooler than mid- and low-latitude oceans, they are still warmer than our estimated temperature thresholds (0.44 °C), particularly where data are currently available (3.35 ± 1.72 °C).⁹ Theoretically, a signal from enzymatic $\text{NO}_3^- - \text{NO}_2^-$ isotope exchange should be present at this temperature, albeit weakly. In this context, besides environmental factors, the key

enzyme NXR, which drives the isotopic exchange, must be considered. NXR is a membrane-associated enzyme with two distinct phylogenetic types.^{69,70} One is the cytoplasmic NXR, found in *Nitrobacter*, *Nitrococcus* and *Nitrolanceus*,⁷¹ while the other type is the periplasmic NXR, found in *Nitrospira* and *Nitrospina*.^{72–75} Both types of NXR belong to the complex iron–sulfur–molybdenum enzyme family (CISM)^{15,75} and consist of three subunits: NxrA (α), NxrB (β), and NxrC (γ).^{14,73} The cytoplasmic NXR is associated with cytosolic nitrate reductase (NAR),^{69,76} whereas the periplasmic NXR is more closely related to type II enzymes of the dimethyl sulfoxide (DMSO) reductase family.^{69,73,74} The periplasmic NXR oxidizes $-\text{NO}_2^-$ to $-\text{NO}_3^-$ in the periplasmic space while hydrolyzing water molecules, generating a proton-driven potential that provides energy to the respiratory chain through ATP and NADH production. In contrast, the cytoplasmic NXR relies on an electron transport protein to first transport NO_2^- into the cell, where it is then oxidized to produce ATP and NADH for cellular metabolism.⁶⁹ NOBs with cytoplasmic NXR require energy to transport NO_2^- and NO_3^- across the cytoplasmic membrane, potentially creating a physiological bottleneck⁶⁹ and making them more sensitive to environmental inhibition. The fact that NXR functions differently depending on its location suggests it may also regulate the enzymatic $\text{NO}_3^- - \text{NO}_2^-$ isotopic exchange reaction. Therefore, if such a reaction is present, the NOB species would likely belong to *Nitrobacter*, *Nitrococcus*, and *Nitrosococcus*. *Nitrococcus*, the dominant NOB species in the marine environment,⁷⁷ has been shown to drive enzymatic isotopic exchange reaction at room temperature rather than at specific low temperatures.¹² This implies that differences in NXR function due to varying NOB species may be a factor in the Arctic Ocean, where enzymatic isotopic exchange reaction has not yet been observed despite the relatively low temperatures.⁹ In light of this, we propose that future studies leveraging microbial genomics and ecological analyses should be conducted for further validation.

5. IMPLICATIONS

Our study employs dual isotopes of NO_3^- and NO_2^- to investigate the enzymatic $\text{NO}_3^- - \text{NO}_2^-$ isotopic exchange reaction in the Southern Ocean and the global ocean. We identify the regulatory role of temperature in this enzymatic isotopic exchange reaction, which complements previous understanding that primarily focused on light as the sole

controlling factor in the mechanism of this reaction. Building on this, we predict future patterns of enzymatic isotopic exchange reaction in the Southern Ocean, which have significant implications for the N cycle and its coupling with the carbon cycle in the Southern Ocean. Furthermore, we provide a characterization of the enzymatic isotope exchange reaction in the global ocean, suggesting a fundamental role for the NXR in this process.

The enzymatic $\text{NO}_3^- - \text{NO}_2^-$ isotopic exchange reaction represents a complex process that involves NOBs, which are increasingly recognized as critical yet remain poorly understood in marine environments. Future research should emphasize these bacteria and their key enzymes to develop a more comprehensive understanding of the enzymatic isotopic exchange reaction and its environmental drivers.

■ ASSOCIATED CONTENT

Data Availability Statement

All data supporting the conclusions of this paper are presented in the main text or supporting materials. The original data set is available upon request from the corresponding author.

Supporting Information

The Supporting Information is available free of charge at <https://pubs.acs.org/doi/10.1021/acs.est.5c02246>.

Estimation of minimum nitrogen and maximum oxygen imparted by canonical N cycle; sampling locations in East and West Antarctic waters from 2020 to 2021; ; distribution of temperature, salinity, NO_3^- , NO_2^- , chlorophyll *a*, and dissolved oxygen in the surface layers of East and West Antarctic surface waters; $\delta^{15}\text{N}_{\text{NO}_2}$ and $\delta^{18}\text{O}_{\text{NO}_2}$ correlations with salinity, chlorophyll *a*, and dissolved oxygen in the mixed layer of global oceans (PDF)

■ AUTHOR INFORMATION

Corresponding Author

Min Chen – College of Ocean and Earth Sciences, Xiamen University, Xiamen 361102, P. R. China; orcid.org/0000-0003-0369-694X; Email: mchen@xmu.edu.cn

Authors

Yanguan Chen – College of Ocean and Earth Sciences, Xiamen University, Xiamen 361102, P. R. China; School of Marine Science and Fisheries, Jiangsu Ocean University, Lianyungang 222005, P. R. China

Minfang Zheng – College of Ocean and Earth Sciences, Xiamen University, Xiamen 361102, P. R. China

Complete contact information is available at: <https://pubs.acs.org/10.1021/acs.est.5c02246>

Author Contributions

M.C. and Y.C. designed research; Y.C. and M.Z. performed research; M.C. and Y.C. analyzed data; and M.C. and Y.C. wrote the paper.

Notes

The authors declare no competing financial interest.

■ ACKNOWLEDGMENTS

We greatly appreciate the anonymous reviewer's constructive and thorough comments. The authors extend their gratitude to the captains and crews of R/V *Xuelong* and R/V *Xuelong 2*, as well as Qi Li, for their invaluable assistance in sample

collection. We also acknowledge Junyi Yuan and Yusheng Qiu for their contributions to the laboratory experiments. This research was supported by the Polar Research Institute of China (IRASCC 02-01-01 and IRASCC 01-01-02C), the National Natural Science Foundation of China (41721005, 42306055), and the Natural Science Foundation of Jiangsu Province (BK20230695).

■ REFERENCES

- (1) Moore, C. M.; Mills, M. M.; Arrigo, K. R.; Berman-Frank, I.; Bopp, L.; Boyd, P. W.; Galbraith, E. D.; Geider, R. J.; Guieu, C.; Jaccard, S. L.; Jickells, T. D.; La Roche, J.; Lenton, T. M.; Mahowald, N. M.; Marañón, E.; Marinov, I.; Moore, J. K.; Nakatsuka, T.; Oschlies, A.; Saito, M. A.; Thingstad, T. F.; Tsuda, A.; Ulloa, O. Processes and patterns of oceanic nutrient limitation. *Nat. Geosci.* **2013**, *6*, 701–710.
- (2) Chen, Y. J.; Chen, M.; Chen, J. X.; Fan, L. F.; Zheng, M. F.; Qiu, Y. S. Dual isotopes of nitrite in the Amundsen Sea in summer. *Sci. Total Environ.* **2022**, *843*, No. 157055.
- (3) Chen, Y. J.; Chen, J. X.; Wang, Y.; Jiang, Y.; Zheng, M. F.; Qiu, Y. S.; Chen, M. Sources and transformations of nitrite in the Amundsen Sea in summer 2019 and 2020 as revealed by nitrogen and oxygen isotopes. *Acta Oceanol. Sin.* **2023**, *42*, 16–24.
- (4) Buchwald, C.; Casciotti, K. L. Isotopic ratios of nitrite as tracers of the sources and age of oceanic nitrite. *Nat. Geosci.* **2013**, *6*, 308–313.
- (5) Casciotti, K. L. Nitrogen and oxygen isotopic studies of the marine nitrogen cycle. *Annu. Rev. Mar. Sci.* **2016**, *8*, 379–407.
- (6) Sigman, D. M.; Fripiat, F.; Studer, A. S.; Kemeny, P. C.; Martínez-García, A.; Hain, M. P.; Ai, X.; Wang, X.; Ren, H.; Haug, G. H. The Southern Ocean during the ice ages: a review of the Antarctic surface isolation hypothesis, with comparison to the North Pacific. *Quat. Sci. Rev.* **2021**, *254*, No. 106732.
- (7) Fripiat, F.; Martínez-García, A.; Marconi, D.; Fawcett, S. E.; Kopf, S. H.; Luu, V. H.; Rafter, P. A.; Zhang, R.; Sigman, D. M.; Haug, G. H. Nitrogen isotopic constraints on nutrient transport to the upper ocean. *Nat. Geosci.* **2021**, *14*, 855–861.
- (8) Chen, Y.; Bardhan, P.; Zhao, X.; Zheng, M.; Qiu, Y.; Chen, M. Nitrite cycle indicated by dual isotopes in the northern South China Sea. *J. Geophys. Res.: Biogeosci.* **2021**, *126*, No. e2020JG006129.
- (9) Chen, Y.; Chen, M. Nitrite cycling in warming Arctic and Subarctic waters. *Geophys. Res. Lett.* **2022**, *49*, No. e2021GL096947.
- (10) Kemeny, P. C.; Weigand, M. A.; Zhang, R.; Carter, B. R.; Karsh, K. L.; Fawcett, S. E.; Sigman, D. M. Enzyme-level interconversion of nitrate and nitrite in the fall mixed layer of the Antarctic Ocean. *Glob. Biogeochem. Cycles* **2016**, *30*, 1069–1085.
- (11) Fripiat, F.; Martínez-García, A.; Fawcett, S. E.; Kemeny, P. C.; Studer, A. S.; Smart, S. M.; Rubach, F.; Oleynik, S.; Sigman, D. M.; Haug, G. H. The isotope effect of nitrate assimilation in the Antarctic Zone: Improved estimates and paleoceanographic implications. *Geochim. Cosmochim. Acta* **2019**, *247*, 261–279.
- (12) Buchwald, C.; Wankel, S. D. Enzyme-catalyzed isotope equilibrium: A hypothesis to explain apparent N cycling phenomena in low oxygen environments. *Mar. Chem.* **2022**, *244*, No. 104140.
- (13) Casciotti, K. L. Inverse kinetic isotope fractionation during bacterial nitrite oxidation. *Geochim. Cosmochim. Acta* **2009**, *73*, 2061–2076.
- (14) Sundermeyer-Klinger, H.; Meyer, W.; Warninghoff, B.; Bock, E. Membrane-bound nitrite oxidoreductase of *Nitrobacter*: evidence for a nitrate reductase system. *Arch. Microbiol.* **1984**, *140*, 153–158.
- (15) Meincke, M.; Bock, E.; Kastrau, D.; Kroneck, P. M. H. Nitrite oxidoreductase from *Nitrobacter hamburgensis*: redox centers and their catalytic role. *Arch. Microbiol.* **1992**, *158*, 127–131.
- (16) Granger, J.; Sigman, D. M.; Needoba, J. A.; Harrison, P. J. Coupled nitrogen and oxygen isotope fractionation of nitrate during assimilation by cultures of marine phytoplankton. *Limnol. Oceanogr.* **2004**, *49*, 1763–1773.

- (17) Granger, J.; Sigman, D. M.; Lehmann, M. F.; Tortell, P. D. Nitrogen and oxygen isotope fractionation during dissimilatory nitrate reduction by denitrifying bacteria. *Limnol. Oceanogr.* **2008**, *53*, 2533–2545.
- (18) Buchwald, C.; Casciotti, K. L. Oxygen isotopic fractionation and exchange during bacterial nitrite oxidation. *Limnol. Oceanogr.* **2010**, *55*, 1064–1074.
- (19) Casciotti, K. L.; Böhlke, J. K.; McIlvin, M. R.; Mroczkowski, S. J.; Hannon, J. E. Oxygen isotopes in nitrite: analysis, calibration, and equilibration. *Anal. Chem.* **2007**, *79*, 2427–2436.
- (20) Babbín, A. R.; Buchwald, C.; Morel, F. M. M.; Wankel, S. D.; Ward, B. B. Nitrite oxidation exceeds reduction and fixed nitrogen loss in anoxic Pacific waters. *Mar. Chem.* **2020**, *224*, No. 103814.
- (21) Buchwald, C.; Santoro, A. E.; Stanley, R. H. R.; Casciotti, K. L. Nitrogen cycling in the secondary nitrite maximum of the eastern tropical North Pacific off Costa Rica. *Global Biogeochem. Cycles* **2015**, *29*, 2061–2081.
- (22) Casciotti, K. L.; Buchwald, C.; McIlvin, M. Implications of nitrate and nitrite isotopic measurements for the mechanisms of nitrogen cycling in the Peru oxygen deficient zone. *Deep Sea Res., Part I* **2013**, *80*, 78–93.
- (23) Kalvelage, T.; Lavik, G.; Lam, P.; Contreras, S.; Arteaga, L.; Löscher, C. R.; Oschlies, A.; Paulmier, A.; Stramma, L.; Kuypers, M. M. Nitrogen cycling driven by organic matter export in the South Pacific oxygen minimum zone. *Nat. Geosci.* **2013**, *6*, 228–234.
- (24) Peng, X.; Fuchsman, C. A.; Jayakumar, A.; Warner, M. J.; Devol, A. H.; Ward, B. B. Revisiting nitrification in the Eastern Tropical South Pacific: A focus on controls. *J. Geophys. Res.-Oceans* **2016**, *121*, 1667–1684.
- (25) Tsementzi, D.; Wu, J.; Deutsch, S.; Nath, S.; Rodriguez-R, L. M.; Burns, A. S.; Ranjan, P.; Sarode, N.; Malmstrom, R. R.; Padilla, C. C.; Stone, B. K.; Bristow, L. A.; Larsen, M.; Glass, J. B.; Thamdrup, B.; Woyke, T.; Konstantinidis, K. T.; Stewart, F. J. SAR11 bacteria linked to ocean anoxia and nitrogen loss. *Nature* **2016**, *536*, 179–183.
- (26) Sun, X.; Frey, C.; Ward, B. B. Nitrite Oxidation Across the Full Oxygen Spectrum in the Ocean. *Global Biogeochem. Cycles* **2023**, *37*, No. e2022GB007548.
- (27) Granger, J.; Sigman, D. M. Removal of nitrite with sulfamic acid for nitrate N and O isotope analysis with the denitrifier method. *Rapid Commun. Mass Spectrom.* **2009**, *23*, 3753–3762.
- (28) Bourbonnais, A.; Letscher, R. T.; Bange, H. W.; Échevin, V.; Larkum, J.; Mohn, J.; Yoshida, N.; Altabet, M. A. N₂O production and consumption from stable isotopic and concentration data in the Peruvian coastal upwelling system. *Glob. Biogeochem. Cycles* **2017**, *31*, 678–698.
- (29) Hu, H.; Bourbonnais, A.; Larkum, J.; Bange, H. W.; Altabet, M. A. Nitrogen cycling in shallow low-oxygen coastal waters off Peru from nitrite and nitrate nitrogen and oxygen isotopes. *Biogeosciences* **2016**, *13*, 1453–1468.
- (30) Kobayashi, K.; Fukushima, K.; Onishi, Y.; Nishina, K.; Makabe, A.; Yano, M.; Wankel, S. D.; Koba, K.; Okabe, S. Influence of $\delta^{18}\text{O}$ of water on measurements of $\delta^{18}\text{O}$ of nitrite and nitrate. *Rapid Commun. Mass Spectrom.* **2021**, *35*, No. e8979.
- (31) Strickland, J. D. H.; Parsons, T. R. A Practical Handbook of Seawater Analysis. *Bull. Fish. Res. Bd. Canada* **1972**, *167*, 1–310.
- (32) Dai, M.; Wang, L.; Guo, X.; Zhai, W.; Li, Q.; He, B.; Kao, S.-J. Nitrification and inorganic nitrogen distribution in a large perturbed river/estuarine system: The Pearl River estuary. *China. Biogeosciences* **2008**, *5*, 1227–1244.
- (33) Casciotti, K. L.; Sigman, D. M.; Hastings, M. G.; Böhlke, J. K.; Hillkert, A. Measurement of the oxygen isotopic composition of nitrate in seawater and freshwater using the denitrifier method. *Anal. Chem.* **2002**, *74*, 4905–4912.
- (34) Sigman, D. M.; Casciotti, K. L.; Andreani, M.; Barford, C.; Galanter, M.; Böhlke, J. K. A bacterial method for the nitrogen isotopic analysis of nitrate in seawater and freshwater. *Anal. Chem.* **2001**, *73*, 4145–4153.
- (35) McIlvin, M. R.; Casciotti, K. L. Technical updates to the bacterial method for nitrate isotopic analyses. *Anal. Chem.* **2011**, *83*, 1850–1856.
- (36) McIlvin, M. R.; Altabet, M. A. Chemical conversion of nitrate and nitrite to nitrous oxide for nitrogen and oxygen isotopic analysis in freshwater and seawater. *Anal. Chem.* **2005**, *77*, 5589–5595.
- (37) Granger, J.; Boshers, D. S.; Böhlke, J. K.; Yu, D.; Chen, N.; Tobias, C. R. The influence of sample matrix on the accuracy of nitrite N and O isotope ratio analyses with the azide method. *Rapid Commun. Mass Spectrom.* **2020**, *34*, No. e8569.
- (38) Mitchell, B. G.; Brody, E. A.; Holm-Hansen, O.; McClain, C.; Bishop, J. Light limitation of phytoplankton biomass and macro-nutrient utilization in the Southern Ocean. *Limnol. Oceanogr.* **1991**, *36*, 1662–1677.
- (39) Martin, J. H.; Gordon, R. M.; Fitzwater, S. E. Iron in Antarctic waters. *Nature* **1990**, *345*, 156–158.
- (40) Casciotti, K. L.; Forbes, M.; Vedamati, J.; Peters, B. D.; Martin, T. S.; Mordy, C. W. Nitrous oxide cycling in the Eastern Tropical South Pacific as inferred from isotopic and isotopomeric data. *Deep Sea Res., Part II* **2018**, *156*, 155–167.
- (41) Liu, S.; Ning, X.; Dong, S.; Song, G.; Wang, L.; Altabet, M. A.; Zhu, Z.; Wu, Y.; Ren, J. L.; Liu, C. G.; Zhang, J.; Huang, D. Source versus recycling influences on the isotopic composition of nitrate and nitrite in the East China Sea. *J. Geophys. Res.: Oceans* **2020**, *125*, No. e2020JC016061.
- (42) Santoro, A. E.; Sakamoto, C. M.; Smith, J. M.; Plant, J. N.; Gehman, A. L.; Worden, A. Z.; Johnson, K. S.; Francis, C. A.; Casciotti, K. L. Measurements of nitrite production in and around the primary nitrite maximum in the central California Current. *Biogeosciences* **2013**, *10*, 7395–7410.
- (43) Peng, X.; Fawcett, S. E.; van Oostende, N.; Wolf, M. J.; Marconi, D.; Sigman, D. M.; Ward, B. B. Nitrogen uptake and nitrification in the subarctic North Atlantic Ocean. *Limnol. Oceanogr.* **2018**, *63*, 1462–1487.
- (44) Peters, B. D.; Babbín, A. R.; Lettmann, K. A.; Mordy, C. W.; Ulloa, O.; Ward, B. B.; Casciotti, K. L. Vertical modeling of the nitrogen cycle in the eastern tropical South Pacific oxygen deficient zone using high-resolution concentration and isotope measurements. *Glob. Biogeochem. Cycles* **2016**, *30*, 1661–1681.
- (45) Peters, B.; Horak, R.; Devol, A.; Fuchsman, C.; Forbes, M.; Mordy, C. W.; Casciotti, K. L. Estimating fixed nitrogen loss and associated isotope effects using concentration and isotope measurements of NO₃⁻, NO₂⁻, and N₂ from the Eastern Tropical South Pacific oxygen deficient zone. *Deep Sea Res., Part II* **2018**, *156*, 121–136.
- (46) Kelly, C. L.; Travis, N. M.; Baya, P. A.; Casciotti, K. L. Quantifying nitrous oxide cycling regimes in the eastern tropical North Pacific Ocean with isotopomer analysis. *Global Biogeochem. Cycles* **2021**, *35*, No. e2020GB006637.
- (47) Gluschkoff, N.; Santoro, A. E.; Buchwald, C.; Casciotti, K. L. Shifts in the isotopic composition of nitrous oxide between El Niño and La Niña in the Eastern Tropical South Pacific. *Global Biogeochem. Cycles* **2023**, *37*, No. e2023GB007959.
- (48) Martin, T. S.; Casciotti, K. L. Paired N and O isotopic analysis of nitrate and nitrite in the Arabian Sea oxygen deficient zone. *Deep Sea Res., Part I* **2017**, *121*, 121–131.
- (49) Casciotti, K. L. Nitrite isotopes as tracers of marine N cycle processes. *Philos. Trans. Royal Soc. A* **2016**, *374*, 20150295.
- (50) Tanaka, Y.; Fukumori, Y.; Yamanaka, T. Purification of cytochrome *a₁c₁* from *Nitrobacter agilis* and characterization of nitrite oxidation system of the bacterium. *Arch. Microbiol.* **1983**, *135*, 265–271.
- (51) Ward, B. B. Chapter 5-Nitrification in marine systems. In *Nitrogen in the Marine Environment*; Capone, D. G.; Bronk, D. A.; Mulholland, M. R.; Carpenter, E. J., Eds.; Elsevier Academic Press: Amsterdam, 2008; pp 199–261.
- (52) Olson, R. J. ¹⁵N tracer studies of the primary nitrite maximum. *J. Mar. Res.* **1980**, *39*, 203–226.

- (53) Guerrero, M. A.; Jones, R. D. Photoinhibition of marine nitrifying bacteria. II. Dark recovery after monochromatic or polychromatic irradiation. *Mar. Ecol.: Prog. Ser.* **1996**, *141*, 193–198.
- (54) Vanzella, A.; Guerrero, M. A.; Jones, R. D. Effect of CO and light on ammonium and nitrite oxidation by chemolithotrophic bacteria. *Mar. Ecol.: Prog. Ser.* **1989**, *57*, 69–76.
- (55) Wing, B. A.; Halevy, I. Intracellular metabolite levels shape sulfur isotope fractionation during microbial sulfate respiration. *Proc. Natl. Acad. Sci. U. S. A.* **2014**, *111* (51), 18116–18125.
- (56) Knapp, B. D.; Willis, L.; Gonzalez, C.; Vashistha, H.; Jammal-Touma, J.; Tikhonov, M.; Ram, J.; Salman, H.; Elias, J. E.; Huang, K. C. Metabolic rearrangement enables adaptation of microbial growth rate to temperature shifts. *Nat. Microbiol.* **2025**, *10*, 185–201.
- (57) Knapp, B. D.; Huang, K. C. The effects of temperature on cellular physiology. *Annu. Rev. Biophys.* **2022**, *51*, 499–526.
- (58) Alster, C. J.; Weller, Z. D.; von Fischer, J. C. A meta-analysis of temperature sensitivity as a microbial trait. *Glob Change Biol.* **2018**, *24*, 4211–4224.
- (59) Yu, L.; Li, R.; Mo, P.; Fang, Y.; Li, Z.; Peng, D. Stable partial nitrification at low temperature via selective inactivation of enzymes by intermittent thermal treatment of thickened sludge. *Chem. Eng. J.* **2021**, *418*, No. 129471.
- (60) Gruber, N. Warming up, tipping sour, losing breath: ocean biogeochemistry under global change. *Philos. Trans. Royal Soc. A* **2011**, *369*, 1980–1996.
- (61) Li, X.; Cai, W.-J.; Meehl, G. A.; Chen, D.; Yuan, X.; Raphael, M.; Holland, D. M.; Ding, Q.; Fogt, R. L.; Markle, B. R.; Wang, G.; Bromwich, D. H.; Turner, J.; Xie, S.-P.; Steig, E. J.; Gille, S. T.; Xiao, C.; Wu, B.; Lazzara, M. A.; Chen, X.; Stammerjohn, S.; Holland, P. R.; Holland, M. M.; Cheng, X.; Price, S. F.; Wang, Z.; Bitz, C. M.; Shi, J.; Gerber, E. P.; Liang, X.; Goosse, H.; Yoo, C.; Ding, M.; Geng, L.; Xin, M.; Li, C.; Dou, T.; Liu, C.; Sun, W.; Wang, X.; C. Song, C. Tropical teleconnection impacts on Antarctic climate changes. *Nat. Rev. Earth Environ.* **2021**, *2*, 680–698.
- (62) Schmidtko, S.; Heywood, K. J.; Thompson, A. F.; Aoki, S. Multidecadal warming of Antarctic waters. *Science* **2014**, *346*, 1227–1231.
- (63) Cook, A. J.; Holland, P. R.; Meredith, M. P.; Murray, T.; Luckman, A.; Vaughan, D. G. Ocean forcing of glacier retreat in the western Antarctic Peninsula. *Science* **2016**, *353*, 283–286.
- (64) Pritchard, H. D.; Ligtenberg, S. R.; Fricker, H. A.; Vaughan, D. G.; van den Broeke, M. R.; Padman, L. Antarctic ice-sheet loss driven by basal melting of ice shelves. *Nature* **2012**, *484*, 502–505.
- (65) Bromwich, D. H.; Nicolas, J. P.; Monaghan, A. J.; Lazzara, M. A.; Keller, L. M.; Weidner, G. A.; Wilson, A. B. Central West Antarctica among the most rapidly warming regions on Earth. *Nature Geosci* **2013**, *6*, 139–145.
- (66) IPCC Summary for Policymakers. In *Climate Change 2023: Synthesis Report. Contribution of Working Groups I, II and III to the Sixth Assessment Report of the Intergovernmental Panel on Climate Change* [Core Writing Team, Lee, H.; Romero, J. (eds.)]. IPCC: Geneva, Switzerland, 2023; pp 1–34.
- (67) Zakem, E. J.; Al-Haj, A.; Church, M. J.; van Dijken, G. L.; Dutkiewicz, S.; Foster, S. Q.; Fulweiler, R. W.; Mills, M. M.; Follows, M. J. Ecological control of nitrite in the upper ocean. *Nat. Commun.* **2018**, *9*, 1206.
- (68) Wan, X. S.; Sheng, H.; Dai, M.; Church, M. J.; Zou, W.; Li, X.; Hutchins, D. A.; Ward, B. B.; Kao, S.-J. Phytoplankton-nitrifier interactions control the geographic distribution of nitrite in the upper ocean. *Global Biogeochem. Cycles* **2021**, *35*, No. e2021GB007072.
- (69) Daims, H.; Lückner, S.; Wagner, M. A new perspective on microbes formerly known as nitrite-oxidizing bacteria. *Trends Microbiol.* **2016**, *24*, 699–712.
- (70) Pester, M.; Maixner, F.; Berry, D.; Rattei, T.; Koch, H.; Lückner, S.; Nowka, B.; Richter, A.; Spieck, E.; Lebedeva, E.; Loy, A.; Wagner, M.; Daims, H. *NxrB* encoding the beta subunit of nitrite oxidoreductase as functional and phylogenetic marker for nitrite-oxidizing *Nitrospira*. *Environ. Microbiol.* **2014**, *16*, 3055–3071.
- (71) Sorokin, D. Y.; Lückner, S.; Vejmelkova, D.; Kostrikina, Na. A.; Kleerebezem, R.; Rijpstra, W. C.; Damsté, J. S.; Le Paslier, D.; Muyzer, G.; Wagner, M.; van Loosdrecht, M. M.; Daims, H. Nitrification expanded: discovery, physiology, and genomics of a nitrite-oxidizing bacterium from the phylum *Chloroflexi*. *ISME J.* **2012**, *6*, 2245–2256.
- (72) Spieck, E.; Bock, E. The lithoautotrophic nitrite-oxidizing bacteria. In *Bergey's Manual® of Systematic Bacteriology*; Brenner, D. J.; Krieg, N. R.; Staley, J. T.; Garrity, G. M., Eds.; Springer: New York, 2005; pp149-153.
- (73) Lückner, S.; Wagner, M.; Maixner, F.; Pelletier, E.; Koch, H.; Vacherie, B.; Rattei, T.; Damsté, J. S.; Spieck, E.; Le Paslier, D.; Daims, H. A *Nitrospira* metagenome illuminates the physiology and evolution of globally important nitrite-oxidizing bacteria. *Proc. Natl. Acad. Sci. U.S.A.* **2010**, *107*, 13479–13484.
- (74) Lückner, S.; Nowka, B.; Rattei, T.; Spieck, E.; Daims, H. The genome of *Nitrospina gracilis* illuminates the metabolism and evolution of the major marine nitrite oxidizer. *Front. Microbiol.* **2013**, *4*, 27.
- (75) Rothery, R. A.; Workun, G. J.; Weiner, J. H. The prokaryotic complex iron-sulfur molybdoenzyme family. *Biochim. Biophys. Acta* **2008**, *1778*, 1897–1929.
- (76) Starckenburg, S. R.; Larimer, F. W.; Stein, L. Y.; Klotz, M. G.; Chain, P. S. G.; Sayavedra-Soto, L. A.; Poret-Peterson, A. T.; Gentry, M. E.; Arp, D. J.; Ward, B.; Bottomley, P. J. Complete genome sequence of *Nitrobacter hamburgensis* X14 and comparative genomic analysis of species within the genus *Nitrobacter*. *Appl. Environ. Microbiol.* **2008**, *74*, 2852–2863.
- (77) Levipan, H. A.; Molina, V.; Fernandez, C. *Nitrospina*-like bacteria are the main drivers of nitrite oxidation in the seasonal upwelling area of the Eastern South Pacific (Central Chile ~ 36°S). *Environ. Microbiol. Rep.* **2014**, *6*, 565–573.